PHYSICAL REVIEW B **85**, 201202(R) (2012)

Semiconducting transition-metal oxides based on d^5 cations: Theory for MnO and Fe_2O_3

Haowei Peng and Stephan Lany*
National Renewable Energy Laboratory, Golden, Colorado 80401, USA
(Received 18 January 2012; published 17 May 2012)

Transition-metal oxides with partially filled d shells are typically Mott or charge-transfer insulators with notoriously poor transport properties due to large effective electron/hole masses or due to carrier self-trapping. Employing band-structure calculations and *ab initio* small-polaron theory for MnO and Fe_2O_3, we explore the potential of d^5 oxides for achieving desirable semiconducting properties, e.g., in solar energy applications. The quantification of self-trapping energies and the trends with the coordination symmetry suggest strategies to overcome the main bottlenecks, i.e., the tendency for self-trapping of holes due to Mn(II) and of electrons due to Fe(III).

DOI: 10.1103/PhysRevB.85.201202 PACS number(s): 72.20.−i, 71.38.−k, 71.20.Nr

Most transition-metal (TM) oxides have a semiconducting band gap and strong optical absorption in the visible range, which would make them interesting materials for solar energy conversion, either as photovoltaic or as photoelectrocatalytic absorber materials,[1,2] for the latter of which oxides are particularly attractive due to their better chemical stability in an aqueous environment.[3] However, efficient charge separation in solar absorbers requires also good carrier transport properties,[3] which are often deteriorated in TM oxides either by carrier self-trapping that leads to an unfavorable small-polaron transport mechanism,[4–7] or by high effective masses resulting from narrow d bands.[8] Hematite Fe_2O_3 has specifically been considered as absorber material for photoelectrocatalytic water splitting,[3] but its poor majority carrier (electron) mobility resulting from a small-polaron transport mechanism,[9] as well as the very short minority carrier (hole) lifetime, remain barriers for a desirable performance as a photoanode for water splitting.

Achieving a good hole mobility and conductivity is generally difficult in TM oxides, or even in main group oxides.[7,10] The prototypical p-type oxides are Cu_2O[11] and $CuAlO_2$,[10,12] where p-type conductivity is facilitated by the p-d repulsion between the O-p and Cu-d^{10} shells.[10,11] We explore here the prospects of achieving desirable carrier transport properties by means of a d^5 high-spin configuration in TM oxides, where a similar p-d interaction occurs in the occupied spin channel, considering the prototypical Mn(II) and Fe(III) oxides, MnO and Fe_2O_3. In order to determine band-structure properties, we performed many-body quasiparticle energy calculations in the GW approximation[13] (GW denotes the Green's function G and the screened Coulomb interaction W). In order to determine whether carrier transport occurs in a band or in a small-polaron mechanism, we performed generalized Koopmans calculations,[14,15] which allow a quantitative evaluation of the carrier self-trapping energy. In addition to the octahedrally coordinated rocksalt (RS) ground-state structure of MnO with an antiferromagnetic ordering along the [111] direction, we are considering also the tetrahedrally coordinated zinc-blende (ZB) polymorph[16] with magnetic ordering along the [001] direction. In hematite Fe_2O_3, which has an antiferromagnetic double-layer sequence along the c axis of the hexagonal unit cell,[17] the Fe ion is approximately octahedrally coordinated.

As a reference for the following discussion, Fig. 1(a) shows schematically the molecular orbital interactions of a d^5 cation. In octahedral or tetrahedral coordination, the TM

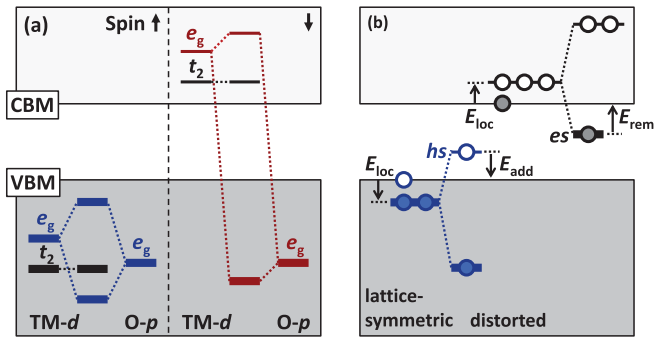

FIG. 1. (Color online) (a) Schematic illustration of the molecular orbital interactions of a d^5 TM cation (occupied orbital levels are shown bold). (b) Illustration of the formation of a hole state (hs) or an electron state (es) inside the band gap due to the formation of a small polaron.

d orbitals split into t_2 (d_{xy},d_{yz},d_{xz}) and e_g ($d_{x^2-y^2}$,d_{z^2}) crystal field symmetries. In the case of the octahedral coordination illustrated in Fig. 1(a), the e_g crystal field state interacts with the same-symmetry state of the oxygen ligands to form bonding and antibonding states, whereas the t_2 symmetry is a nonbonding state.[18] In tetrahedral coordination (not shown), the coupling scheme is similar, only that the t_2 symmetry is interacting and e_g is nonbonding. Figure 1(b) illustrates the formation of a hole state or an electron state inside the gap following the trapping of a carrier into the molecular orbital level that lies closest to the band edge as shown in Fig. 1(a) (see the discussion below).

All electronic structure calculations presented here were performed using the VASP code,[19,20] and for the computational details we refer to the Supplemental Material[21] (see also Refs. 22–27 therein). As a baseline for subsequent GW[13] and generalized Koopmans[14,15] calculations, we perform density-functional calculations using the exchange correlation functional of Ref. 28 in the generalized gradient approximation (GGA) and an on-site Coulomb term[25] with $U = 3$ eV for Mn-d and Fe-d. Keeping the GGA + U wave functions, the GW energies were iterated to self-consistency, where local field effects derived from the local density functional were taken into account. This procedure yields rather reliable predictions for a range of II-VI and III-V main group compounds.[29] Metal d states, however, lie often too high in energy in GW, in both

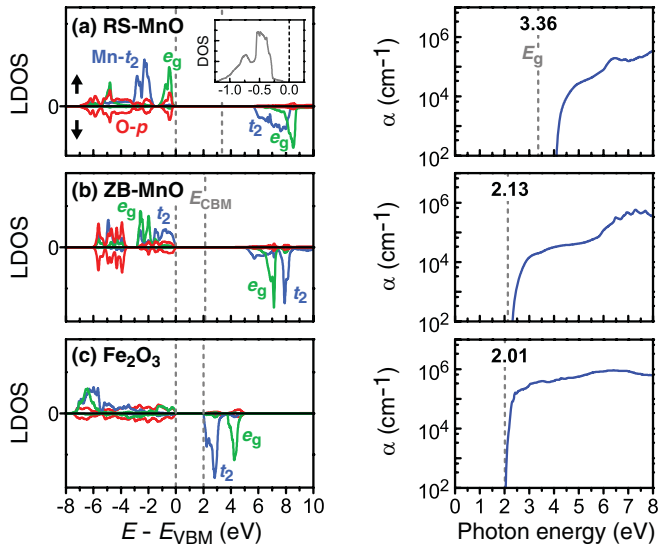

FIG. 2. (Color online) Local density of states and absorption spectrum obtained from many-body *GW* calculations for (a) MnO in the ground-state rocksalt structure, (b) MnO in the zinc-blende polymorph, and (c) hematite Fe_2O_3. The inset in (a) shows the total density of states in the vicinity of the VBM.

cases of occupied shells, such as in ZnO,[30] and unoccupied shells, such as in TiO_2 or in V_2O_5.[31] This problem also accounts for the tendency of common *GW* approaches to overestimate the band gap of Fe_2O_3 that is formed between occupied O-*p* and unoccupied Fe-*d* states.[32] As a remedy, we use here an attractive on-site potential for *d* states in the form of the nonlocal external potentials.[33] By comparison with the experimental band gap energies for MnO (3.4 eV), Mn_3O_4 (2.5 eV), FeO (2.1 eV), and Fe_2O_3 (2.1 eV),[34] we find that no such correction is necessary for Mn, but a potential of $V_d = -2.0$ eV is needed for Fe to reconcile experiment and the *GW* prediction. Our results for RS-MnO are very similar to that of previous *GW* calculations.[35]

Figure 2 shows the local density of states (LDOS) and the respective absorption spectra for the two polymorphs of MnO and for Fe_2O_3 based on the *GW* quasiparticle energies. The band-structure features (i.e., the t_2/e_g splitting) anticipated in Fig. 1 are clearly discernible in Fig. 2. Table I gives the *GW* band gaps and the carrier effective masses. The usual band effective mass is given for electrons in MnO. Due to nonparabolicity and/or anisotropy of the hole masses, and the electron mass in Fe_2O_3, in these cases we give the equivalent effective mass[31] obtained from the integration of the density of states weighted with a Boltzmann distribution at 300 K.

TABLE I. Fundamental band gaps (E_g), electron effective masses (m_e^*/m_e), and hole effective masses (m_h^*/m_e) for the two polymorphs of MnO and in Fe_2O_3 from *GW* calculations (Ref. 21).

	E_g (eV)	m_e^*/m_e	m_h^*/m_e
RS-MnO	3.36	0.3	1.2
ZB-MnO	2.13	0.3	4.8
Fe_2O_3	2.01	1.5	2.1

Interestingly, MnO has a highly dispersive *s*-like conduction band, similar to, say, ZnO, where the unoccupied Mn-*d* orbitals lie rather far above the conduction band minimum (CBM) [cf. Figs. 2(a) and 2(b)]. The resulting light effective electron mass suggests excellent electron transport properties in both polymorphs of MnO. The band gap of 2.1 eV in the ZB structure is significantly smaller than the indirect gap of the RS phase, and the overlap of the absorption spectrum with the solar spectrum suggests that MnO could be an interesting solar material if the ZB phase can be stabilized. In Fe_2O_3, the CBM is formed by the unoccupied t_2 symmetries of Fe-*d* [cf. Fig. 2(c)], whose high density of states leads to a very sharp onset of strong optical absorption above the (slightly indirect) band gap, but also causes a relatively heavy electron mass (Table I). Thus, improving the electron transport properties of Fe_2O_3 would require increasing the conduction band dispersion, thereby reducing the large effective mass. This strategy would be also beneficial in view of self-trapping and small-polaron transport for electrons (see below).

Returning to the concept of *p*-*d* repulsion as a means to improve hole transport, we now discuss the hole effective masses. The smallest effective hole mass of $m_h^*/m_e = 1.2$ is found for RS-MnO. In this structure, the Mn-d_{z^2} and $d_{x^2-y^2}$ sublevels of the e_g manifold have lobes pointing directly toward the O ligands, causing a strong *p*-*d* interaction [cf. Fig. 1(a)], which leads to a strong valence band dispersion and low DOS in the vicinity of the valence band maximum (VBM) [cf. Fig. 2(a) inset]. In the tetrahedral coordination of Mn in the ZB polymorph, the *p*-*d* interaction occurs in the t_2 symmetry. Here, however, the respective Mn-d_{xy}, d_{yz}, and d_{xz} orbitals do not point directly toward the O neighbors (see also below in the context of polarons), leading to a weaker interaction and, hence, to a larger effective mass of $m_h^*/m_e = 4.8$. Similar to Mn in RS-MnO, Fe in Fe_2O_3 is approximately octahedrally coordinated, but the energy of the Fe-d^5 shell lies significantly lower in energy [see Fig. 2(c)], again leading to a weaker *p*-*d* interaction than in RS-MnO and a higher mass of $m_h^*/m_e = 2.1$ (see Table I). Nevertheless, all hole masses obtained here are comparable to that of the prototypical *p*-type oxide Cu_2O ($m_h^*/m_e = 3.7$),[31] and still much lower than in many other binary or ternary TM oxides (the respective calculated values for m_h^*/m_e are 17.0, 10.0 and 18.0 in FeO, $CuAlO_2$[31] and Co_2ZnO_4,[36] respectively). Thus, the *p*-d^5 interaction is a promising concept for TM oxides with good hole transport properties.

Besides having suitable band-structure properties such as band gap, absorption, and effective masses, a solar absorber material needs further to be robust against carrier *self-trapping*, which not only leads to a small-polaron transport mechanism with notoriously low carrier mobilities,[37] but also causes deep defect states inside the band gap that can act as effective recombination centers leading to short minority carrier lifetimes. Carrier self-trapping is the result of the localization of an electron or hole at a specific lattice location, forming an electron state (es) or hole state (hs) inside the band gap [cf. Fig. 1(b)]. Formally, this process can be described as a change of the oxidation state of the ion at which the electron or hole state is localized, e.g., $Fe^{+III} + e^- \rightarrow Fe^{+II}$,[9] or $Mn^{+II} + h^+ \rightarrow Mn^{+III}$,[7] and $O^{-II} + h^+ \rightarrow O^{-I}$.[38]

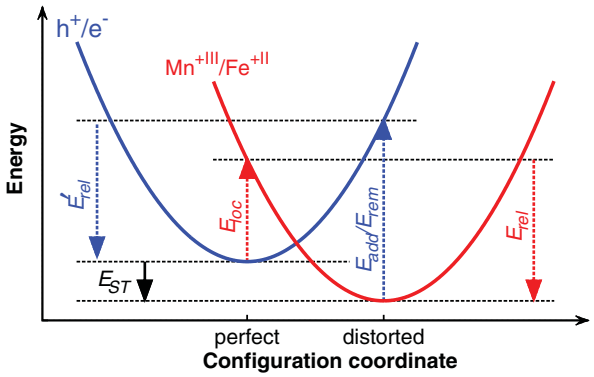

FIG. 3. (Color online) The schematic configuration coordinate energy diagram for self-trapping of an excess hole in MnO and an excess electron in Fe_2O_3. h^+ (e^-) denotes a hole (an electron) at the VBM (CBM), whereas Mn^{+III} (Fe^{+II}) denotes the respective self-trapped state.

For an illustration of the self-trapping process, we plot in Fig. 3 a schematic configuration coordinate diagram. The self-trapping energy

$$E_{ST} = E_{loc} + E_{rel}, \tag{1}$$

can be decomposed[39] into a localization energy $E_{loc} > 0$ for exciting a carrier from the delocalized bandlike state (e^- or h^+) into the respective resonant molecular orbital level [cf. E_{loc} in Fig. 1(b)], and a relaxation energy $E_{rel} < 0$ which stabilizes the localized polaronic state (e.g., Mn^{+III} or Fe^{+II}).

Theoretical predictions of the self-trapping energy within a first-principles framework have been hampered by the bias of local density (LD) calculations to favor delocalized solutions and the bias of the Hartree-Fock (HF) approach to favor localized solutions.[40] Thus, even though the electron transfer involved in small-polaron hopping in Fe_2O_3 has been studied in great detail using quantum chemical methods,[9] few quantitative predictions for E_{ST} are presently available.[41,42] We here employ the density-functional based approach of Refs. 14 and 15 where the delocalization bias is removed by enforcing a generalized Koopmans condition that restores the correct linear variation of the energy with respect to the fractional electron number.[40]

In the context of the present polaron calculations, the generalized Koopmans condition states that for a self-trapped hole, the electron addition energy E_{add} should equal the Kohn-Sham single-particle energy of the *initially unoccupied* hole state, i.e., $E(N+1) - E(N) = e_{hs}(N)$. In order to make this condition satisfied, we introduced in Ref. 14 a parametrized on-site potential

$$V_{hs} = \lambda_{hs}(1 - n_{m,\sigma}/n_{host}) \tag{2}$$

for O-p-like hole states (O^{-I} polarons), where $n_{m,\sigma}$ is the partial charge of the m sublevel of spin σ, n_{host} is the O-p partial charge of the unperturbed host material, and λ_{hs} is a parameter that is adjusted to match the generalized Koopmans condition. For TM-d derived hole states, such as Mn^{+III} in MnO, we apply V_{hs} of the same form as Eq. (2). Since we aim to recover the true quasiparticle energy of the unoccupied hole state relative to the spectrum of the occupied valence band states, we define the reference occupation $n_{host} = 0.94$ by the average Mn-d partial charge of the occupied majority spin direction ("arrow up" in Fig. 2).

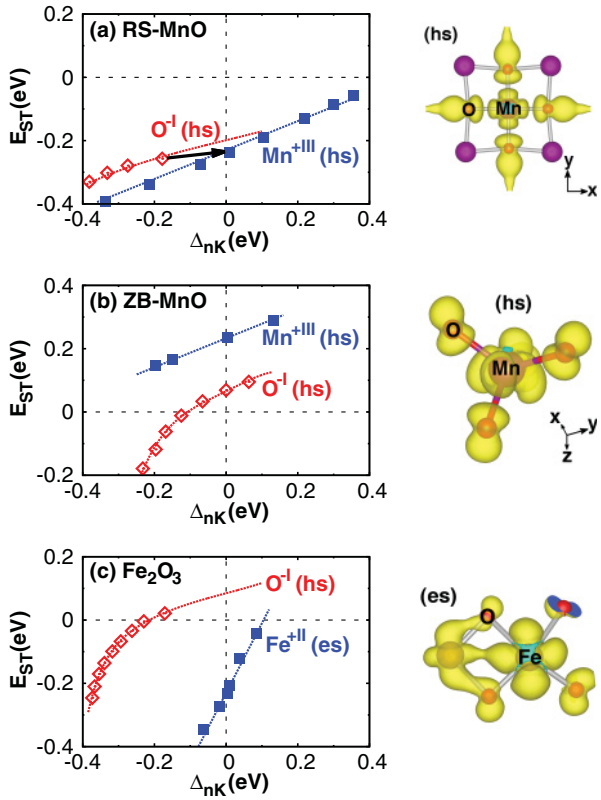

FIG. 4. (Color online) Left: The calculated self-trapping energy E_{ST} as a function of the non-Koopmans energy Δ_{nK}, for (a) RS-MnO, (b) ZB-MnO, and (c) Fe_2O_3. Right: Isosurface plot[43] of the squared wave functions of the Mn^{+III} hole states in (a) RS-MnO, and in (b) ZB-MnO, and for the Fe^{+II} electron state in (c) Fe_2O_3.

To describe correctly the energy of occupied electron states relative to the spectrum of unoccupied conduction band states, we now define a reference p_{host} that measures the degree to which the d symmetries that form the CBM are empty, using the definition $p_{m,\sigma} = 1 - n_{m,\sigma}$. The electron state potential analogous to Eq. (2) is then given by

$$V_{es} = \lambda_{es}(p_{m,\sigma}/p_{host} - 1). \tag{3}$$

For the Fe_2O_3, we determine $p_{host} = 0.90$ from the partial charge of the Fe d-t_2 states of the unoccupied minority spin direction which form the CBM [cf. Fig. 2(c)]. The corresponding generalized Koopmans condition for a self-trapped electron is that the electron removal energy E_{rem} should equal the negative single-particle energy of the *initially occupied* electron state, $E(N-1) - E(N) = -e_{es}(N)$.

The generalized Koopmans calculations were performed using a supercell approach, where the appropriate finite-size corrections for total energies[26] and single-particle energies[27] e_{hs} and e_{es} of charged cells have been taken into account (see Supplemental Material[21]). Figure 4 shows the self-trapping energy E_{ST} as a function of the non-Koopmans energy $\Delta_{nK} = E_{add} - e_{hs}$ or $\Delta_{nK} = e_{es} - E_{rem}$, which measures the bias toward delocalization ($\Delta_{nK} > 0$ as in LD) or localization ($\Delta_{nK} < 0$ as in HF). We find that under the correct condition $\Delta_{nK} = 0$, holes self-trap as Mn^{+III} in RS-MnO with a negative

TABLE II. The calculated self-trapping energy E_{ST} for the Mn^{+III} hole states and the Fe^{+II} electron state in MnO and Fe_2O_3, and the decomposition of E_{ST} into E'_{loc} and E'_{rel} [cf. Eqs. (1) and (4)].

Polaron in system	E_{ST} (eV)	E'_{rel} (eV)	E'_{loc} (eV)
Mn^{+III} (hs) in RS-MnO	−0.24	−0.88	+0.64
Mn^{+III} (hs) in ZB-MnO	+0.23	−0.64	+0.87
Fe^{+II} (es) in Fe_2O_3	−0.23	−0.29	+0.06

$E_{ST} = -0.24$ eV, but not in ZB-MnO where $E_{ST} = +0.23$ eV is positive. Electrons self-trap as Fe^{+II} in Fe_2O_3 with $E_{ST} = -0.23$ eV. The respective parameters in Eqs. (2) and (3) are $\lambda_{hs} = 5.6$ eV, $\lambda_{hs} = 6.5$ eV, and $\lambda_{es} = 0.1$ eV in RS-MnO, ZB-MnO, and Fe_2O_3, respectively [in Fe_2O_3, GGA + U already satisfies Eq. (3) in good approximation].

We now discuss the physical origin of the carrier self-trapping phenomenology in terms of the decomposition of the self-trapping energy into E_{loc} and E_{rel} [Eq. (1)]. The direct calculation of E_{loc}, which is always positive for self-trapped states,[5] is, however, difficult due to the resonant character of the state inside the continuum of host bands [cf. Fig. 1(b)]. Thus, we determine instead an approximated localization energy E'_{loc},

$$E'_{loc} = E_{ST} - E'_{rel}, \tag{4}$$

which equals E_{loc} if the energy gain E_{rel} upon lattice distortion following carrier trapping equals the energy gain E'_{rel} upon restoration of the perfect lattice following the carrier release into the respective band edge (see Fig. 3). (Note that in case of defect bound polarons, where E_{loc} can be negative, it was indeed observed that the two atomic relaxation energies involved in the carrier capture/release cycle are comparable.[14,15,44]) The result of this analysis is given in Table II.

Addressing the question why self-trapping of Mn^{+III} holes is avoided in ZB-MnO, we observe the following: First, E'_{loc} in the RS structure is smaller than in the ZB structure, because the Mn-e_g resonance in RS-MnO peaks closer to VBM [cf. Fig. 2(a)] than the Mn-t_2 resonance in ZB-MnO [cf. Fig. 2(b)]; second, the relaxation energy E'_{rel} stabilizes the polaronic state in the RS structure more than in the ZB structure, which is related to the fact that the Mn-e_g derived hole state of $d_{x^2-y^2}$ symmetry points directly toward the O ligands [cf. Fig. 4(a)], whereas the Mn-t_2 derived hole state of d_{xy} symmetry does not [cf. Fig. 4(b)] and therefore interacts less strongly with the ligands. In Fe_2O_3, the Fe^{+II} electron state shows a much smaller relaxation energy compared to the Mn^{+III} hole state, mainly due to the *nonbonding* t_2 character of the electron state [cf. Fig. 1(a)]; the very small localization energy results from the high Fe-t_2 LDOS at energies just above the CBM [cf. Fig. 2(c)].

We further calculated the O^{-I} polarons which were found to be important in TiO_2,[8,42] but we found that E_{ST} is positive in ZB-MnO and Fe_2O_3, and that the O^{-I} state decays into the Mn^{+III} state in RS-MnO, as denoted by the arrow in Fig. 4(a). Considering Mn^{+I} electron states in MnO and Fe^{+IV} hole states in Fe_2O_3, we could not identify configurations that could lead to negative self-trapping energies. In view of the fact that the main resonances of the unoccupied Mn-d states in the conduction band and of the occupied Fe-d states in the valence band are separated from the band edge energies by several eV (cf. Fig. 2), we expect rather large localization energies for Mn^{+I} electron states and Fe^{+IV} hole states, which are unlikely to be overcome by the relaxation energy.

Summarizing the results of our calculations, we find that both MnO and Fe_2O_3 have strongly hybridized valence bands due to the p-d^5 coupling, which leads to an increased valence band dispersion and—for a transition-metal (TM) oxide—relatively small effective hole masses. The d^5 cations Mn^{+II} and Fe^{+III} exhibit an interesting asymmetry in regard of their carrier trapping behavior: Mn^{+II} tends to trap holes but not electrons, whereas Fe^{+III} tends to trap electrons but not holes. Thus, electrons in MnO and holes in Fe_2O_3 are expected to show bandlike transport, but RS-MnO and Fe_2O_3 are predicted to be small-polaron conductors for holes and electrons, respectively. In ZB-MnO, self-trapping is inhibited due to the tetrahedral coordination of Mn. Thus, our study provides specific directions for avoiding the detrimental effects of poor carrier mobility and short minority carrier lifetimes due to self-trapping. In Mn oxides, hole self-trapping could be avoided by stabilizing the tetrahedral coordination of Mn in ternary oxides or in alloys. In Fe_2O_3, the quantitative prediction of the self-trapping energy enables approaches for band-structure design aiming to lower the CBM energy below the Fe^{+II} electron-trap level whose energy position we have determined here quantitatively. The experimental realization of such d^5 TM oxides with improved transport properties is in progress.

This work is supported by the US Department of Energy, Office of Science, Office of Basic Energy Sciences, Energy Frontier Research Centers, under Contract No. DE-AC36-08GO28308 to NREL. The high performance computing resources of the National Energy Research Scientific Computing Center and of NREL's Computational Science Center are gratefully acknowledged. We thank T. R. Paudel, A. Zunger, A. Zakutayev, N. H. Perry, and T. O. Mason for interest and stimulating discussions on the problem of small-polaron conductivity.

*Stephan.Lany@nrel.gov

[1] H. Zhang, G. Chen, and D. W. Bahnemann, J. Mater. Chem. **19**, 5089 (2009).

[2] C. Wadia, A. P. Alivisatos, and D. M. Kammen, Environ. Sci. Technol. **43**, 2072 (2009).

[3] K. Sivula, F. Le Formal, and M. Graetzel, ChemSUSChem **4**, 432 (2011).

[4] D. Emin, Phys. Today **35**, 34 (1982).

[5] L. D. Landau, Phys. Z. Sowjetunion **3**, 664 (1933).

[6] A. M. Stoneham, J. Chem. Soc., Faraday Trans. 2 **85**, 505 (1989).

[7] J. M. Honig, in *Basic Properties of Binary Oxides*, edited by A. Dominguez-Rodriguez, J. Castaing, and R. Marquez (University of Seville Press, Seville, 1984), p. 101.

[8] A. R. Nagaraja, N. H. Perry, T. O. Mason, Y. Tang, M. Grayson, T. R. Paudel, S. Lany, and A. Zunger, J. Am. Ceram. Soc. **95**, 269 (2012).
[9] K. M. Rosso, D. M. A. Smith, and M. Dupuis, J. Chem. Phys. **118**, 6455 (2003); N. Iordanova, M. Dupuis, and K. M. Rosso, *ibid.* **122**, 144305 (2005).
[10] H. Kawazoe, M. Yasukawa, H. Hyodo, M. Kurita, H. Yanagi, and H. Hosono, Nature (London) **389**, 939 (1997).
[11] H. Raebiger, S. Lany, and A. Zunger, Phys. Rev. B **76**, 045209 (2007).
[12] J. Tate, H. L. Ju, J. C. Moon, A. Zakutayev, A. P. Richard, J. Russell, and D. H. McIntyre, Phys. Rev. B **80**, 165206 (2009).
[13] L. Hedin, Phys. Rev. **139**, A796 (1965).
[14] S. Lany and A. Zunger, Phys. Rev. B **80**, 085202 (2009).
[15] S. Lany, Phys. Status Solidi B **248**, 1052 (2011).
[16] A. Schrön, C. Rödl, and F. Bechstedt, Phys. Rev. B **82**, 165109 (2010).
[17] C. G. Shull, E. O. Wollan, and W. C. Koehler, Phys. Rev. **84**, 912 (1951).
[18] Note that in O_h symmetry, the six p_m suborbitals of the O ligands that point toward the cation site form a_1, t_1, and e_g crystal field states, so e_g is the only common representation: J. Osorio-Guillen, S. Lany, S. V. Barabash, and A. Zunger, Phys. Rev. Lett. **96**, 107203 (2006); I. S. Elfimov, S. Yunoki, and G. A. Sawatzky, *ibid.* **89**, 216403 (2002).
[19] G. Kresse and J. Hafner, Phys. Rev. B **47**, 558 (1993); **49**, 14251 (1994).
[20] M. Shishkin and G. Kresse, Phys. Rev. B **74**, 035101 (2006).
[21] See Supplemental Material at http://link.aps.org/supplemental/10.1103/PhysRevB.85.201202 for details of calculation.
[22] P. E. Blöchl, Phys. Rev. B **50**, 17953 (1994).
[23] G. Kresse and D. Joubert, Phys. Rev. B **59**, 1758 (1999).
[24] H. J. Monkhorst and J. D. Pack, Phys. Rev. B **13**, 5188 (1976).
[25] S. L. Dudarev, G. A. Botton, S. Y. Savrasov, C. J. Humphreys, and A. P. Sutton, Phys. Rev. B **57**, 1505 (1998).
[26] S. Lany and A. Zunger, Phys. Rev. B **78**, 235104 (2008).
[27] S. Lany and A. Zunger, Phys. Rev. B **81**, 113201 (2010).
[28] J. P. Perdew, K. Burke, and M. Ernzerhof, Phys. Rev. Lett. **77**, 3865 (1996).
[29] S. Lany, M. d'Avezac, P. Graf, and A. Zunger (unpublished).
[30] M. Shishkin, M. Marsman, and G. Kresse, Phys. Rev. Lett. **99**, 246403 (2007).
[31] G. Trimarchi, H. Peng, J. Im, A. J. Freeman, V. Cloet, A. Raw, and K. R. Poeppelmeier, K. Biswas, S. Lany, and A. Zunger, Phys. Rev. B **84**, 165116 (2011).
[32] P. Liao and E. A. Carter, Phys. Chem. Chem. Phys. **13**, 15189 (2011).
[33] S. Lany, H. Raebiger, and A. Zunger, Phys. Rev. B **77**, 241201(R) (2008).
[34] T. Usani and T. Masumi, Physica B + C **86-88**, 985 (1977); H. Y. Xu, S. L. Xu, X. D. Li, H. Wang, and H. Yan, Appl. Surf. Sci. **252**, 4091 (2006); H. K. Bowen, D. Adler, and B. H. Auker, J. Solid State Chem. **12**, 355 (1975); I. Balberg and H. L. Pinch, J. Mag. Magn. Mater. **7**, 12 (1978).
[35] S. V. Faleev, M. van Schilfgaarde, and T. Kotani, Phys. Rev. Lett. **93**, 126406 (2004); C. Rödl, F. Fuchs, J. Furthmüller, and F. Bechstedt, Phys. Rev. B **79**, 235114 (2009).
[36] J. D. Perkins, T. R. Paudel, A. Zakutayev, P. F. Ndione, P. A. Parilla, D. L. Young, S. Lany, D. S. Ginley, A. Zunger, N. H. Perry, Y. Tang, M. Grayson, T. O. Mason, J. S. Bettinger, Y. Shi, and M. F. Toney, Phys. Rev. B **84**, 205207 (2011).
[37] A. J. Bosman and H. J. van Daal, Adv. Phys. **19**, 1 (1970).
[38] O. F. Schirmer, J. Phys.: Condens. Matter **23**, 334218 (2011).
[39] E. N. Heifets and A. L. Shluger, J. Phys. Condens. Matter. **4**, 8311 (1992).
[40] J. P. Perdew, A. Ruzsinszky, G. I. Csonka, O. A. Vydrov, G. E. Scuseria, V. N. Staroverov, and J. Tao, Phys. Rev. A **76**, 040501(R) (2007).
[41] D. Munoz Ramo, A. L. Shluger, J. L. Gavartin, and G. Bersuker, Phys. Rev. Lett. **99**, 155504 (2007).
[42] B. J. Morgan and G. W. Watson, Phys. Rev. B **80**, 233102 (2009).
[43] Figures produced with VESTA: K. Momma and F. Izumi, J. Appl. Crystallogr. **44**, 1272 (2011).
[44] S. Lany and A. Zunger, Phys. Rev. B **81**, 205209 (2010).